Raman scattering study of δ-BiB$_3$O$_6$ crystal

E. A. Strikina, A. S. Krylov, A. S. Oreshonkov & A. N. Vtyurin

Taylor & Francis
Taylor & Francis Group

Raman scattering study of δ-BiB$_3$O$_6$ crystal

E. A. Strikina[a], A. S. Krylov[a,b], A. S. Oreshonkov[a,b], and A. N. Vtyurin[a,b]

[a]Kirensky Institute of Physics, SB RAS, Krasnoyarsk, Russia; [b]Siberian Federal University, Krasnoyarsk, Russia

ABSTRACT

The total set of polarized Raman spectra have been obtained at room temperature, and an assignment of observed modes based on the lattice dynamics simulation and polarization selection rules is proposed. An LO-TO splitting of A$_1$ Raman bands have been observed.

Introduction

The phase diagram of Bi$_2$O$_3$-B$_2$O$_3$ system had been studied intensively in sixties [1], and the crystal of bismuth triborate BiB$_3$O$_6$ synthesized among them for the first time. This crystal attracted a special interest of several scientific groups in the last years due to its high optical nonlinearity that provides wide practical applications as an active medium in systems of optical frequency transformations. For a long time only one α-phase was known for this composition, but six new phases of BiB$_3$O$_6$ have been found in the recent years [2]. However, only α-phase investigated in details up to now. A structure of the α-phase is built of chains of [BO$_3$] triangles and [BO$_4$] tetrahedrons in 1:2 ratio. First principles simulations of its electronic structure showed that [BO$_4$] tetrahedrons provide the main part of optical nonlinearity. Among other phases of BiB$_3$O$_6$ only γ and δ include [BO$_4$] tetrahedrons exclusively; and centrosymmetrical γ phase is of scanty interest for nonlinear optics, while the structure of δ phase ($Pca2_1$, $Z = 4$) looks more attractive for such applications. The structure of the δ-BiB$_3$O$_6$ is shown in Fig. 1, the experimental cell parameters and atomic coordinates can be taken from [3].

The ab initio calculations of the phonon spectra, dielectric and elastic properties of the γ and δ modifications of the BiB$_3$O$_6$ crystal have been published in [4]. The vibrational spectra and lattice dynamics calculations of δ-BiB$_3$O$_6$ have been published earlier in [5], however, not for all possible polarization directions. In this work, we have performed such measurements.

Experimental

Samples for experiments were taken from the same crystallization as in [6]. The spectra in the backscattering geometry were recorded with Horiba Jobin Yvon T64000 spectrometer equipped with a liquid nitrogen cooled charge coupled with the device detection system in

---
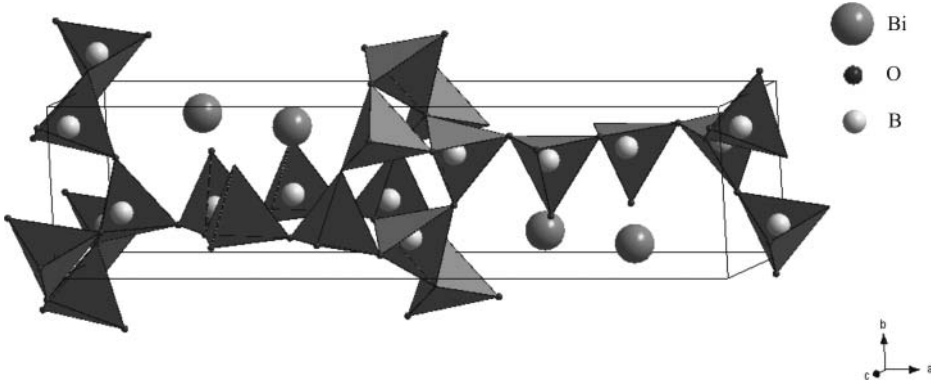
Figure 1. The crystal structure of the δ–BiB$_3$O$_6$ crystal.

subtractive dispersion mode in 10 to 1600 cm^{-1} range. Ar$^+$ ion laser Spectra Physics Stabilite 2017 with $\lambda = 514.5$ nm and power 3 mW on a sample was used as an excitation light source. The experiments were carried out using incident laser beam focused on the sample by 50x Olympus MPlan objective lens with a numerical aperture (NA) of 0.75. The scattered light was collected by the same objective lens in the backscattering geometry and analyzed through a polarizer and λ-plate. To investigate the low-wavenumber spectra, spectroscopic measurements were performed in the subtractive dispersion mode, which attained a low wavenumber limit of 4 cm^{-1} in the present setup. The deformation of the low wavenumber spectral edge by an optical slit, which sometimes smears the true features of low wavenumber spectra, was carefully eliminated by rigorous optical alignment. We use the standard notation [7] to describe the geometry of Raman scattering.

Results and discussion

The vibrational representation of the $Pca2_1$ orthorhombic phase at Brillouin zone center of BiB$_3$O$_6$ crystal is: $\Gamma_{\text{Vibr}} = 30A_1 + 30A_2 + 30B_1 + 30B_2$, acoustic and optic modes: $\Gamma_{\text{acoustic}} = A_1 + B_1 + B_2$, $\Gamma_{\text{optic}} = 29A_1 + 30A_2 + 29B_1 + 29B_2$, Raman and Infrared active modes: $\Gamma_{\text{Raman}} = 29A_1(aa, bb, cc) + 30A_2 (ab, ba) + 29B_1(ac, ca) + 29B_2(bc, cb)$, $\Gamma_{\text{Infrared}} = 29A_1 + 29B_1 + 29B_2$. Corresponding components of the Raman scattering tensor are given in brackets.

Fig. 2 shows Raman spectra for all possible polarization directions in which A_1 and A_2 modes are active (diagonal components of Raman tensor). LO–TO splitting for A_1 mode can be clearly seen from Fig. 2a and 2b. Raman bands corresponding to B_1 and B_2 modes presented in Fig 3a and 3b.

To simulate the δ-BiB$_3$O$_6$ vibrational the spectrum package LADY [8] was used. Complete spectra of the δ-BiB$_3$O$_6$ crystal obtained within the framework of common model of 'rigid-ion', where interatomic potential is considered as a sum of long range Coulomb electrostatic:

$$V^{\text{RIM}}(r_{ij}) = \frac{1}{2}\sum_{ij}\frac{Z_iZ_j}{r_{ij}} + U(r_{ij}), \tag{1}$$
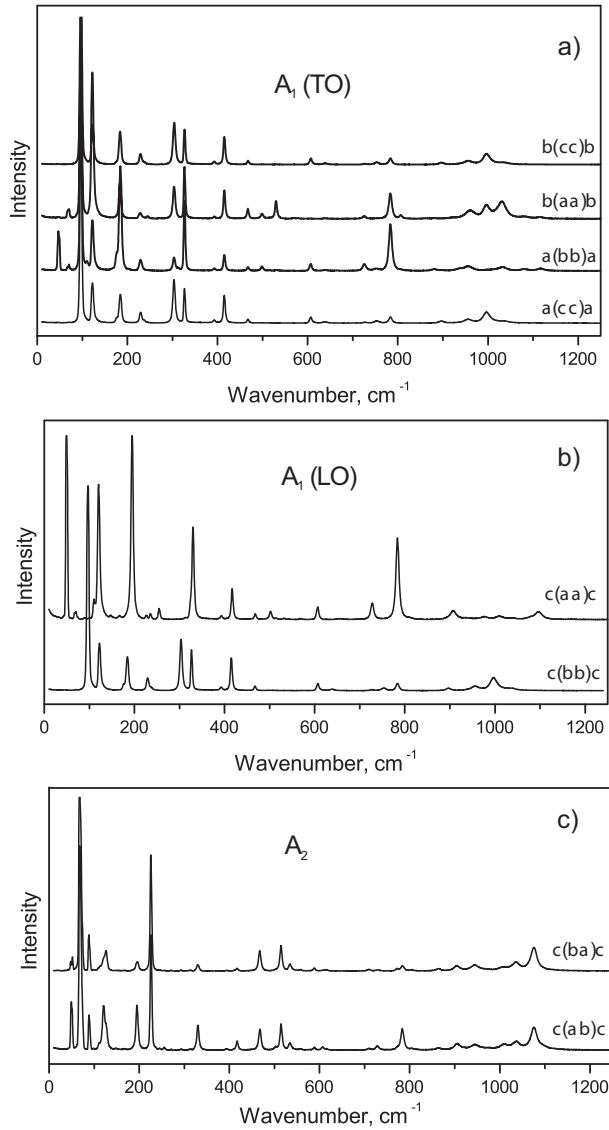
Figure 2. Raman spectra of the δ–BiB$_3$O$_6$ crystal at: a) *b(cc)b, b(aa)b, a(bb)a, a(cc)a* b) *c(aa)c, c(bb)c,* c) *c(ba) c, c(ab)c* geometries.

and the short-range interaction potential was taken in the Born–Mayer form:

$$U(r_{ij}) = \lambda \exp(-r_{ij}/\rho), \tag{2}$$

where r_{ij} is the interatomic distance and λ and ρ are the parameters characterizing of the short-range pair interionic interaction. Resulting model parameters were obtained by minimization of residual values of the simulated and experimental Raman frequencies using the Fletcher – Reeves method [9–11]. The values of λ, ρ and Z_{ij} are listed in Table 1. Calculated values of Raman active modes are shown in Table 2 in comparison with experimental results.
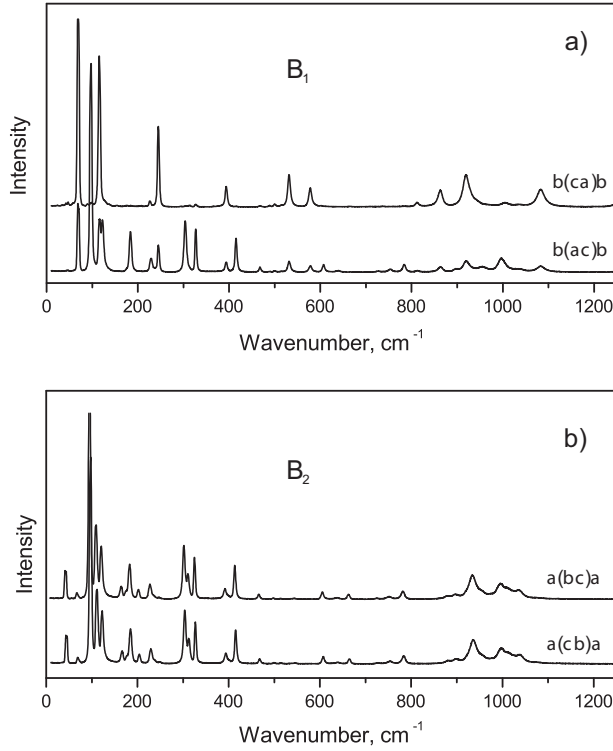
Figure 3. Raman spectra of the δ–BiB_3O_6 crystal at: a) $a(bc)a$ b) $a(cb)a$

In the case of the ideal BO_4 tetrahedron, only normal symmetric stretching ν_1 and antisymmetric stretching ν_3 vibrations should appear in the range of > 650 cm^{-1} [12]. However, taking into account the fact that the atoms in δ-BiB_3O_6 are in general positions, the B–O distances are different and BO_4 tetrahedrons interconnected to each other, their normal internal modes should be distorted. For this reason the considered spectral region and the whole spectrum is rich in lines of BO_4 tetrahedra. Our simulations show that about 40 Raman active modes in the range of >650 cm^{-1} should appear at different polarization geometries. Bands in the 350–650 cm^{-1} range are assigned to the distorted ν_2 and ν_4 BO_4 bending modes. Generally, frequency of ν_4 vibration should be above that of ν_2 vibration [12]. The lower wavenumber range of 150–350 cm^{-1} contains translational, rotational and mixed vibrations of BO_4 tetrahedra. The bands below 150 cm^{-1} are assigned to Bi translation vibrations.

Table 1. Parameters of the interatomic interaction potential.

Interactions	Radii of interaction, Å	λ, aJ/Å^2	ρ, Å
Bi – O	0–3.00	350.00	0.300
B1 – O	0–1.50	321.60	0.210
B2 – O	0–1.60	400.60	0.220
B3 – O	0–1.60	345.30	0.199
O – O	0–3.00	242.80	0.245
Ion	Bi	B	O
Z(e)	2.00	1.80	−1.2333

Table 2. Experimental and calculated Raman frequencies of the δ–BiB_3O_6 crystal.

A$_1$ exp. TO	A$_1$ exp. LO	A$_1$ calc.	A$_2$ exp.	A$_2$ calc.	B$_1$ exp.	B$_1$ calc.	B$_2$ exp.	B$_2$ calc.
1116	1097	1121	1076	1153		1212		1278
1081	1035	1093	1037	1119	1082	1132	1037	1132
1031	1007	979	1010	1090	1035	1023	1010	1029
996	975	959	978	981	997	949	997	965
959	935	908	944	945	955	938	956	929
919	907	894	905	912	919	910	936	905
864	865	789	864	805	897	854	880	892
807	783	752	784	755	863	803	784	786
783	727	721	728	751	813	749	727	737
752	650	697	709	730	783	732	665	689
726	607	634	607	648	753	648	607	647
639	530	598	558	606	727	618	515	623
606	515	552	534	553	607	575	499	563
530	502	510	514	529	578	533	468	518
499	467	490	501	511	531	504	415	483
467	416	447	466	490	515	497	393	459
415	394	428	417	428	500	432	327	442
393	329	384	393	416	467	421	312	400
328	310	345	330	382	415	392	304	383
303	256	320	313	332	394	347	249	338
272	244	274	255	310	327	319	226	307
228	235	255	246	262	304	299	204	280
186	225	221	226	227	245	267	185	240
175	194	159	196	191	229	229	177	185
122	165	128	126	170	184	156	166	135
97	120	100	110	94	123	116	123	119
71	88	69	89	89	116	89	112	94
67	69	46	68	70	97	76	98	66
46	49	18	51	54	71	55	69	35
			49	44	68		45	

Conclusions

The experimental Raman spectra of δ-BiB_3O_6 crystal for all possible polarizations are obtained. The number of spectral lines are in the agreement with the vibrational representation, polarization selection rules and lattice dynamics simulations. Observed Raman bands are assigned to corresponding vibrational modes based on the lattice dynamics simulations.

Funding

References

1. E. M. Levin and C. L. McDaniel, The system Bi_2O_3-B_2O_3. *J. Am. Ceram. Soc.* **45**, 355–360, (1962).
2. Rihong Cong, Jinlong Zhu, Yingxia Wang, Tao Yang, Fuhui Liao, Changqing Jin and Jianhua Lin, Phase transitions among four BiB_3O_6 polymorphs: a detailed investigation. *Cryst. Eng. Comm.* **11**, 1971–1978, (2009).

3. J. S. Knyrim, P. Becker, D. Johrendt and H. Huppertz, A New Non-Centrosymmetric Modification of BiB_3O_6. *Angew. Chem. Int. Ed.* **45**, 8239–8241, (2006).
4. M. S. Pavlovskii, A. S. Shinkorenko and V. I. Zinenko, Calculation of lattice dinamics, elastic and Dielectric Properties of γ-BiB_3O_6 and δ-BiB_3O_6. *Physics of the Solid State.* **57**, 675–682, (2015).
5. M. Maczka, L. Macalik and A. Majchrowski, Phonons in nonlinear optical δ-BiB_3O_6 crystal: Raman and infrared spectra and lattice dynamics. *Journal of Alloys and Compounds.* **575**, 86–89, (2013).
6. A. S. Aleksandrovsky, A.D. Vasiliev, A. I. Zaitsev and A. V. Zamkov, Growth, optical and electromechanical properties of single-crystalline orthorhombic bismuth triborate. *Journal of Crystal Growth.* 4027–4030, (2008).
7. D. L. Rousseau, R. P. Bauman and S. P. S. Porto, Normal Mode Determination in Crystals. *J. Raman Spectrosc.* **10**, 253–290, (1981).
8. M. B. Smirnov and V.Yu. Kazimirov, *LADY: software for lattice dynamics simulations.* (JINR communications, Dubna, 2001).
9. A. S. Krylov, A. N. Vtyurin, A. S. Oreshonkov, V. N. Voronov and S. N. Krylova, Structural transformations in a single-crystal Rb_2NaYF_6: Raman scattering study. *J. Raman Spectr.* **44**, 763–770, (2013).
10. Y. V. Gerasimova, A. S. Oreshonkov, A. N. Vtyurin, A. A. Ivanenko, L. I. Isaenko, A. A. Ershov and E. I. Pogoreltsev, Infrared Absorption Investigation of the Role of Octahedral Groups upon the Phase Transition in the $Rb_2KMoO_3F_3$ Crystal. *Phys. Solid State.* **55**, 2331–2334, (2013).
11. Z. Xia, M. S. Molokeev, A. S. Oreshonkov, V. V. Atuchin, Ru-Shi Liu and Cheng Dong, Crystal and local structure refinement in $Ca_2Al_3O_6F$ explored by X-ray diffraction and Raman spectroscopy. *Phys. Chem. Chem. Phys.* **16**, 5952–5957, (2014).
12. K. Nakomoto, *Infrared and Raman Spectra of Inorganic and Coordination Compounds.* (Wiley, New York etc., 2009).